

Modularity and directionality in genetic interaction maps

Ariel Jaimovich^{1,2,†}, Rutu Rinott^{1,†}, Maya Schuldiner^{3,*}, Hanah Margalit^{2,*}
and Nir Friedman^{1,4,*}

¹School of Computer Science and Engineering, The Hebrew University of Jerusalem, Jerusalem 91904, ²Department of Microbiology and Molecular Genetics, IMRIC, Faculty of Medicine, The Hebrew University of Jerusalem, Jerusalem 91120, ³Department of Molecular Genetics, Weizmann Institute of Science, Rehovot 76100 and ⁴The Alexander Silberman Institute of Life Sciences, The Hebrew University of Jerusalem, Jerusalem 91904, Israel

ABSTRACT

Motivation: Genetic interactions between genes reflect functional relationships caused by a wide range of molecular mechanisms. Large-scale genetic interaction assays lead to a wealth of information about the functional relations between genes. However, the vast number of observed interactions, along with experimental noise, makes the interpretation of such assays a major challenge.

Results: Here, we introduce a computational approach to organize genetic interactions and show that the bulk of observed interactions can be organized in a hierarchy of modules. Revealing this organization enables insights into the function of cellular machineries and highlights global properties of interaction maps. To gain further insight into the nature of these interactions, we integrated data from genetic screens under a wide range of conditions to reveal that more than a third of observed aggravating (i.e. synthetic sick/lethal) interactions are unidirectional, where one gene can buffer the effects of perturbing another gene but not vice versa. Furthermore, most modules of genes that have multiple aggravating interactions were found to be involved in such unidirectional interactions. We demonstrate that the identification of external stimuli that mimic the effect of specific gene knockouts provides insights into the role of individual modules in maintaining cellular integrity.

Availability: We designed a freely accessible web tool that includes all our findings, and is specifically intended to allow effective browsing of our results (<http://compbio.cs.huji.ac.il/GIAnalysis>).

Contact: maya.schuldiner@weizmann.ac.il;
hanahm@ekmd.huji.ac.il; nir@cs.huji.ac.il

Supplementary information: Supplementary data are available at *Bioinformatics* online.

1 INTRODUCTION

A major goal in biology is to understand how thousands of genes act together to create a functional cellular environment. An emerging powerful strategy for investigating functional relations between genes involves high-throughput genetic interaction maps (Butland *et al.*, 2008; Byrne *et al.*, 2007; Collins *et al.*, 2007a; Fiedler *et al.*, 2009; Makhnevych *et al.*, 2009; Pan *et al.*, 2006; Roguev *et al.*, 2008; Schuldiner *et al.*, 2005; Segrè *et al.*, 2005; Tong *et al.*, 2001; Wilmes *et al.*, 2008), which measure the extent by which a mutation in one gene modifies the phenotype of a mutation in another. The interactions in these maps can be divided to *alleviating interactions*, where the defect of the double mutant is less than expected from

two independent effects, and *aggravating interactions*, where the defect of the double mutant is greater than expected from the single-gene perturbations. Such systematic mapping typically uncovers a large number of observed genetic interactions, which confounds straightforward interpretation. Despite the large number of published maps, a systematic methodology for extracting biological insights remains a major challenge.

Previous analyses of genetic interaction data have primarily focused on hierarchical clustering, resulting in many new discoveries in key cellular processes (Collins *et al.*, 2007a; Pan *et al.*, 2006; Schuldiner *et al.*, 2005). Nonetheless, hierarchical clustering has two major drawbacks: first, the similarity score between genes is based on their entire interaction profile (with all other genes) allowing large fraction of background interactions to dominate the similarity. Second, it does not directly extract meaningful groups of genes or interactions between such groups, preventing a system-level view of the interaction map. Both challenges were addressed by several methods. For example, the PRISM algorithm (Segrè *et al.*, 2005) uses monochromatic interactions (i.e. solely aggravating or solely alleviating) within and between groups of genes to define pathways (Fig. 1A). However, this algorithm, which was evaluated on simulated interaction maps, fails on actual data from large-scale maps due to the added complexity in real cellular systems and assay noise (data not shown). Biclustering is another approach that was suggested as an alternative to hierarchical clustering, aiming to identify local signatures of functional modules in the genetic interaction maps (Pu *et al.*, 2008). While this approach identifies many modules of genes, it does not eliminate their overlap, hampering the generation of one coherent network structure describing both the intra- and inter-modular interactions. One possible way to overcome these drawbacks is by adding different types of data or additional constraints. For example, methods that combine physical protein–protein interactions in the analysis of genetic interaction data identify functional modules with high precision (Bandyopadhyay *et al.*, 2008; Kelley and Ideker, 2005; Ulitsky *et al.*, 2008). However, the requirement for physical interaction data limits such approaches to protein sets and organisms where such data exist, and may miss many functional pathways that are not mediated by protein complexes (e.g. metabolic pathways).

Here, we introduce an automated approach that builds a concise representation of large-scale genetic interaction maps. Toward this goal, we relied on previous observations that complexes and pathways induce signatures in the form of monochromatic cliques and bi-cliques (Fig. 1A; Beyer *et al.*, 2007; Boone *et al.*, 2007; Segrè *et al.*, 2005). Our method seeks to find an organization that is globally coherent, in the sense that genes are organized into a hierarchy of modules. Moreover, our method requires that the

*To whom correspondence should be addressed.

†The authors wish it to be known that, in their opinion, the first two authors should be regarded as joint First authors.

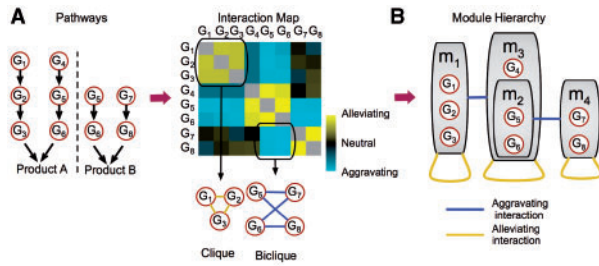


Fig. 1. Modularity of genetic interactions. (A) Pathway architecture (left) leads to expected patterns of genetic interactions between genes (right). Each row/column represents the genetic interactions of a specific gene with all other genes. Among these there are subsets of interactions that can be represented as monochromatic cliques and bicliques. (B) Monochromatic interactions can be captured by edges within and between modules (grey boxes) organized in a hierarchical structure.

interactions between these modules will account for a large portion of the data. We show how the resulting representation facilitates better understanding of the underlying cellular phenomena. In turn, we use these insights to shed light on the function of concrete cellular pathways and also to provide information on the overall organization of the network. We demonstrate how integration of data from genetic screens for reduced fitness under various conditions results in automatic creation of biological insights into the functional role of gene modules.

2 HIERARCHY OF INTERACTING MODULES

Our basic premise is that a good hierarchical organization is defined by a trade-off between succinct description of the network on one hand, and capturing as much of the interactions in the map on the other hand. To capture this quality, we devised a score based on the minimum description length (MDL) principle (Rissanen, 1983) and devised an iterative procedure that optimizes this score.

2.1 Hierarchical representation

The hierarchical representation consists of two parts. The first is a hierarchy of modules. Briefly, a hierarchy is a set \mathcal{M} of *modules*, such that each module m is associated with a subset of genes $\text{Genes}(m)$ and a parent module $\text{Parent}(m) \in \mathcal{M} \cup \{\epsilon\}$, where ϵ represents a null module (i.e. the module is a root). We say that a module m' is an *ancestor* of m if $m' = \text{Parent}^k(m)$ for some $k \geq 1$. The hierarchy is legal if for every $m, m' \in \mathcal{M}$ such that $m' = \text{Parent}(m)$, we have that $\text{Genes}(m) \subset \text{Genes}(m')$, and moreover $\text{Genes}(m) \cap \text{Genes}(m') \neq \emptyset$ if and only if m is an ancestor of m' or vice versa. In the hierarchy of Figure 1B, we have four modules, so that $\text{Genes}(m_1) = \{G_1, G_2, G_3\}$, $\text{Genes}(m_2) = \{G_5, G_6\}$, $\text{Genes}(m_3) = \{G_4, G_5, G_6\}$, and $\text{Genes}(m_4) = \{G_7, G_8\}$. In this example, $\text{Parent}(m_1) = \text{Parent}(m_3) = \text{Parent}(m_4) = \epsilon$, and $\text{Parent}(m_2) = m_3$.

The second component of the hierarchy describes a set \mathcal{E} of *edges* between modules. An edge can be of two types, alleviating (denoted in yellow in our figures) or aggravating (denoted in blue). Each edge represents a type of genetic interactions that is common for the members of the modules linked by the edge. Formally, an edge $m_1 \leftrightarrow m_2$ represent the set $\text{Int}(m_1 \leftrightarrow m_2) = \text{Genes}(m_1) \times \text{Genes}(m_2)$ of genetic interactions. Edges in the hierarchy can be self-edges,

in which case they induce a clique of interactions, or between two different modules in which case they induce a bi-clique of interactions. In the example of Figure 1B, we have the alleviating edges $m_1 \leftrightarrow m_1$, $m_3 \leftrightarrow m_3$, $m_4 \leftrightarrow m_4$, and the aggravating edges $m_1 \leftrightarrow m_3$ and $m_2 \leftrightarrow m_4$. These edges represent the interactions described in the interaction matrix of Figure 1A.

2.2 Minimal description length score

We use the MDL principle (Rissanen, 1983) to score the quality of module hierarchy as a guide for lossless encoding of the genetic interaction map. Conceptually, imagine that we need to transmit the genetic interaction map over a channel and search for the encoding that would require the fewest bits. Under this principle, the length of the transmission is a proxy for the quality of the representation, with a shorter encoding denoting a better representation.

The application of this principle involves deciding how we encode the interactions in the map. When we do not have any organization of the map, we use the same codebook for each interaction. Since weak interactions are much more abundant than strong ones, their code words will be shorter (Cover and Thomas, 2001). Thus, we will incur a penalty for strong interactions. When we have a module hierarchy, we can use a different codebook for each edge in the hierarchy and an additional codebook for background interactions. This allows us to exploit a group of monochromatic interactions for efficient encoding by a codebook that assigns strong interactions of the appropriate short codewords. The benefit from covering a large portion of the map with coherent edges is offset by the cost of transmitting the codebooks themselves, which involves coding the hierarchical organization and the edges with their signs. Thus, when evaluating a possible organization of the genetic interaction map there is a trade-off between the coverage of interactions and the number of modules and edges.

Formally, if we denote the genetic interaction map by D and the hierarchical organization by $(\mathcal{M}, \mathcal{E})$ then the MDL score consists of two main terms:

$$S(D; \mathcal{M}, \mathcal{E}) = \text{DL}(\mathcal{M}, \mathcal{E}) + \text{DL}(D | \mathcal{M}, \mathcal{E})$$

where $\text{DL}(\mathcal{M}, \mathcal{E})$ is the description length of the hierarchical organization and $\text{DL}(D | \mathcal{M}, \mathcal{E})$ is the description length of the interactions, given that we already encoded the hierarchy. We start with the first term, $\text{DL}(\mathcal{M}, \mathcal{E})$. Here, we need to encode the module hierarchy (which module is the parent of each module), the assignment of genes to modules and the list of edges. This is a relatively straightforward encoding using standard MDL practices.

The second term represents how to describe the genetic interaction map once we know the modular organization. Standard results in information theory (Cover and Thomas, 2001) show that if the frequency of each word is $p(w)$, then the optimal codebook is one where encoding a word w is of length $-\log_2 p(w)$. Thus, in each codebook we use the distribution of the strengths of interactions covered by an edge to build an efficient codebook. We assume that the different values are distributed according to a Gaussian distribution. Thus, the encoding length is the minus log-probability (or likelihood) of the data given the parameters of each Gaussian codebook (i.e. the closer the distribution is to its parametric description, the score is higher). To this length, we add the number of bits needed to encode the parameters of each distribution. To calculate the encoding length, for each edge $e \in \mathcal{E}$ we estimate the

maximum likelihood parameters, (μ_e, σ_e) . In addition, we estimate the background distribution (μ_b, σ_b) . We then define

$$\begin{aligned} \text{DL}(D|\mathcal{M}, \mathcal{E}) = & - \sum_{e \in \mathcal{E}} \sum_{(i,j) \in \text{Int}(e)} \log_2 p(I_{i,j}|\mu_e, \sigma_e) \\ & - \sum_{(i,j) \in \text{Bg}} \log_2 p(I_{i,j}|\mu_b, \sigma_b) \\ & + \sum_{e \in \mathcal{E}} \log_2 |\text{Int}(e)| + \log_2 |\text{Bg}| \end{aligned}$$

where $p(I_{i,j}|\mu, \sigma)$ is the likelihood of the genetic interaction score $I_{i,j}$ according to the Gaussian $N(\mu, \sigma^2)$, Bg is the set of interactions that do not belong to any edge in \mathcal{E} , and $\log_2(|\text{Int}(e)|)$ is the encoding length of the parameters for the edge. Thus, we score interactions in their specific context (either inside an edge or in the background).

For practical concerns, we restrict the network to include only coherent edges. Thus, we require that an edge satisfies $|\mu_e| - \sigma_e > \alpha$, where α is a strictness parameter (which we set to 1 in the results below). If this is not the case, the network receives a large penalty which effectively excludes it from consideration.

2.3 Constructing module hierarchy

Given a genetic interaction map D , we want to find the module hierarchy that minimizes the MDL score. This problem is non-trivial as the search space is huge. To address this we combine two ideas. First, we use hierarchical clustering to get a good initial guess for our hierarchical organization. Second, once we have a reasonable initial candidate, a heuristic search procedure can perform ‘local’ improvements to find a much better one. Our procedure implements these ideas by performing the following steps.

Clustering: we cluster the genetic interaction map using hierarchical clustering with uncentered Pearson correlation (Eisen *et al.*, 1998). This results in a dendrogram, which in our terminology is a detailed hierarchy, where each internal node defines a group of genes that correspond to the leaves in its sub-tree and each pair of such internal nodes defines a rectangle in the clustered matrix (Fig. 2a).

Identifying edges: treating the dendrogram as an initial hierarchy of modules, the procedure traverses overall pairs of internal nodes in the dendrogram and in a greedy fashion adds modules and edges as long as they increase the MDL score. At this stage, we have a very large number of modules and some number of edges. We then prune modules that do not participate in edges (while maintaining the ancestral relationships between the remaining modules). This results in a hierarchy that summarizes the initial clustering (Fig. 2b).

Greedy improvements: to re-evaluate and refine the modular structure, the procedure performs a heuristic search by evaluating local changes to the modular organization. These local changes include: addition/removal of a gene to/from an existing module, merging a module with its parent, transferring an edge from a module to its parent (or vice-versa) and addition/removal of an edge. Each of these local changes is evaluated and based on their score the procedure decide which one to apply. We use a best-first-search heuristic combined with a TABU list (Glover *et al.*, 1993) to avoid revisiting explored networks and thus escape local maxima. This search leads to a refined model (Fig. 2c).

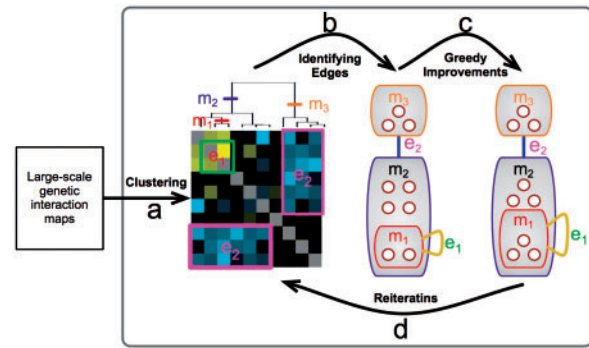


Fig. 2. Outline of our iterative algorithm. After clustering the interactions (left) our procedure identifies modules of genes in the clustering hierarchy that define monochromatic on-diagonal squares (e_1) and off-diagonal rectangles (e_2), resulting in a hierarchical organization of genes into modules (middle). Next, the module graph is refined by a series of local changes (e.g. moving one gene from m_2 to m_1 ; right). At the end of each iteration (bottom arrow), we re-cluster the genetic interaction matrix while maintaining the identified modules. These steps are iterated until convergence.

Reiterations: to find structures that might elude local search steps, the procedure iterates by returning to the first step. In each iteration, we re-cluster the genetic interaction map while conserving the module hierarchy from the previous step. That is, we allow only agglomerative steps that do not break existing modules into separate subunits. This constraint forces the resulting clustering to maintain the found structure, but it can identify new sub-modules as well as new modules of genes that are not assigned to a module. These iterations are repeated until convergence (in score) (Fig. 2d).

2.4 Application to genetic interaction maps in *Saccharomyces cerevisiae*

We applied our methodology to two large-scale genetic interaction maps in the budding yeast *S. cerevisiae*. The first contains genes localized to the Early Secretory Pathway (ESP; Schuldiner *et al.*, 2005) and the other comprises genes involved in Chromosome Biology (CB; Collins *et al.*, 2007b). This procedure automatically constructed a hierarchical organization of modules in both: in the ESP map it identified 113 modules covering 264 genes (out of 424) and in the CB map it identified 242 modules covering 487 genes (out of 743). Most of these modules represent functionally coherent groups of genes (ESP: 76/113, CB: 193/242; Appendix A in the Supplementary website), such as physical complexes (e.g. Mediator subunits, HIR complex, SAS complex) and functional pathways (e.g. *N*-linked glycosylation, chromatid cohesion). Inter- and intra-module interactions correspond to a large fraction of the interactions in the original maps, particularly the high confidence ones (Fig. 3A and B). In addition, the edges we capture are also coherent in the sense that most interactions covered by alleviating edges have positive interaction scores and most interactions covered by aggravating edges have negative scores (Fig. 3C and D). Thus, the modular organization of the genetic interactions faithfully captures a large portion of these maps.

The hierarchical nature of the network allows the definition of large modules with more general functions that contain sub-modules with more specific functions, which are distinguished by sets of unique interactions. For example, module ESP-98 comprises eight

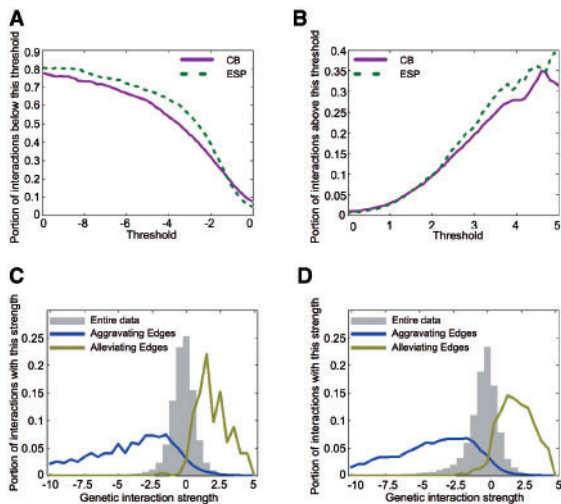


Fig. 3. Edges capture most interactions. (A) Coverage of aggravating interactions by our network (y-axis) as a function of threshold for EMAP score (x-axis). Magenta solid lines and green dashed lines show results for CB and ESP networks, respectively. (B) Coverage of alleviating interactions. (C) Coherence of aggravating and alleviating edges in the CB network. Shown is a histogram (y-axis) of EMAP scores (x-axis) for interactions covered by aggravating and alleviating edges in blue and yellow, respectively. Histogram for the entire data is shown in grey. (D) Coherence of edges in our ESP network.

genes that take part in the maturation of glycoproteins within the ER lumen (Fig. 4). Specifically, these genes encode the sequential enzymes adding on sugar moieties to a synthesized polysaccharide chain. Our analysis identified two sub-modules that correspond to two distinct stages in this process: one module (ESP-97) involves genes encoding proteins that transfer mannose residues to the nascent chain, and the second module (ESP-96) involves genes that subsequently transfer glucose residues to the nascent chain (Helenius and Aebi, 2004). This division was obtained automatically, based on interactions that are specific to each of these sub-modules (Fig. 4). Notably, the protein products of genes in these two modules do not form physical complexes, and thus could not be identified by methods that use protein–protein interactions to define the modules. In addition, this subdivision was not obtained by solely applying hierarchical clustering methods (Schuldiner *et al.*, 2005).

2.5 Comparison to other methods

Comparing our method to previous methods for analysing genetic interaction maps is difficult due to the different focus of the various methods. A common theme to most methods is the determination of gene modules. Although this is only one aspect of our analysis, we compared our module list to modules found by other studies of the CB map (Bandyopadhyay *et al.*, 2008; Pu *et al.*, 2008; Ulitsky *et al.*, 2008). Comparing to the methods of Bandyopadhyay *et al.* (2008) and Ulitsky *et al.* (2008, Fig. 5A and B), we find many more modules (242 modules compared with 91 and 62, respectively), covering more genes (487 genes compared with 374 and 313, respectively).¹ In addition, many of these modules are

¹When comparing to Bandyopadhyay *et al.* (2008) we considered only modules with more than one gene.

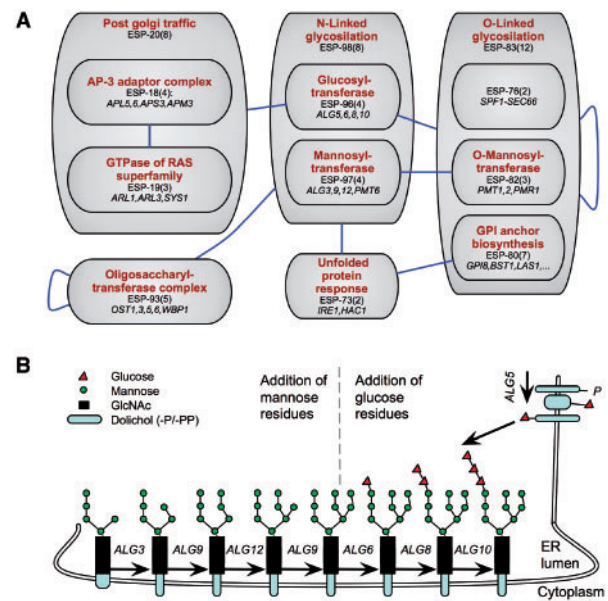


Fig. 4. Hierarchical organization of modules represents functional hierarchy. (A) Modules are denoted by grey boxes (red labels denote functional assignment based on annotations; black labels denote the name of each module and in parentheses the number of genes included in it). Blue edges between modules indicate that these modules create aggravating bicliques. Module ESP-98 contains eight genes related to N-linked glycosylation. It is further divided into two sub-modules (ESP-96 and ESP-97), each identified by different interactions, which have more specific functions. (B) Schematic view of the N-linked glycosylation pathway (adapted from Helenius and Aebi, 2004). Inside the ER lumen, four mannose residues (green circles) are added to Man5GlcNAc2 by Alg3, Alg9 and Alg12 (comprising module ESP-97). In turn, three glucose residues (red triangles) are added by Alg5, Alg6, Alg8 and Alg10 (comprising module ESP-96).

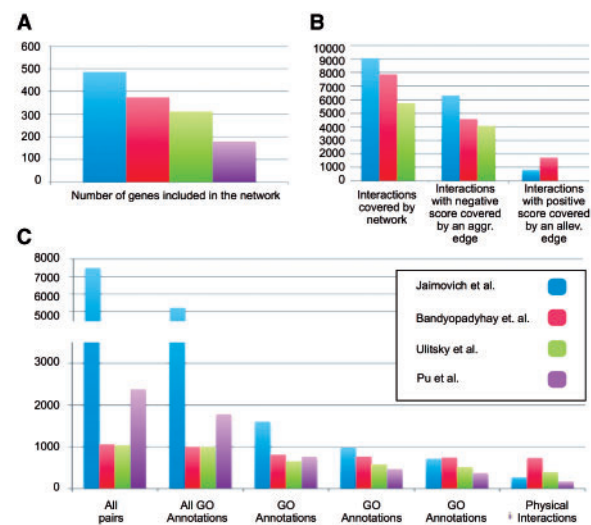


Fig. 5. Comparison to other methods: bar charts showing how many genes (A) and interactions (B) are covered by each method. (C) Bar chart showing how many of the protein pairs that are in the same module share a GO function annotation, or physically interact with each other. GO annotations are divided into categories according to the number of genes in the annotation.

not enriched with physical protein–protein interactions, yet have a coherent function. Furthermore, our approach is also applicable to other systems, in which the protein–protein interaction data is very sparse (such as in the ESP dataset) or in organisms in which it does not exist. When comparing our results to those of Pu *et al.* (2008) who finds 298 overlapping modules covering 181 genes, we see that we find similar numbers of modules organized in a global hierarchy and covering more genes. However, these advantages come at the price of lower precision (Fig. 5C). Yet, as the larger modules at the top of the hierarchy might correspond to more global functions, their enrichment in more general GO terms is reasonable. We conclude that each of the methods strikes a different trade off between precision, sensitivity and global coherence.

3 UNCOVERING UNIDIRECTIONAL COMPENSATION

Strikingly, a relatively large number of the gene pairs exhibit genetic interactions, especially aggravating ones. We find that aggravating interactions play a major role in the definition of many modules (e.g. 150 of the 242 modules in the CB network are defined solely based on aggravating interactions). Aggravating interactions are commonly interpreted as an indication of bidirectional compensation, where each gene can compensate for the absence of the other by performing a similar function. However, in many cases this explanation cannot account for the observed patterns of aggravating interactions and the large number of such interactions between genes with distantly related functions.

An alternative explanation (Boone *et al.*, 2007; Pan *et al.*, 2006) is that one gene is crucial for functions that compensate for the abnormal cellular state resulting from the loss of the other gene. In this scenario, termed *unidirectional compensation*, the relationship between the genes is asymmetric in the sense that one gene can compensate for the loss of the other but not vice versa. We refer to the gene whose knockout causes the perturbation as the *upstream gene* and to the compensating gene as the *downstream gene*. While examples for this type of interpretation have been shown on existing data (Pan *et al.*, 2006), no systematic test was carried out to identify the aggravating interactions that can be explained by such unidirectional interpretation and to assess their fraction within the observed aggravating interactions.

3.1 Identifying unidirectional compensation

Our premise is that we can identify unidirectional compensation by comparing the perturbation of a putative upstream gene with perturbations caused by external stimuli. We say that an external stimulus (e.g. a drug or an environmental insult) *phenocopies* a gene deletion if the genes required for coping with the stimulus are the same ones required to compensate for the perturbation of the upstream gene. Stated in terms of available data, this definition implies a significant overlap between the genes whose knockout lead to sensitivity to the stimulus and these that have aggravating interactions with the upstream gene. Moreover, genes in this overlap are downstream to the specific upstream gene. By establishing such phenocopy relations, we implicate unidirectional interactions from the upstream genes and their matching downstream genes.

For example, deletion of the *CHL1* gene leads to abnormal chromosome segregation similar to the damage caused by external

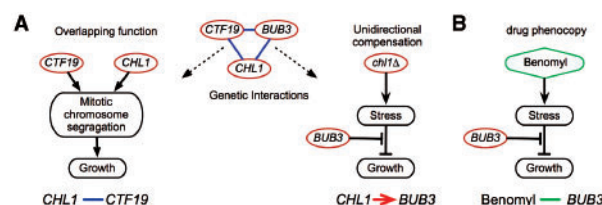


Fig. 6. Identifying unidirectional interactions. (A) An example of aggravating interactions (middle) that might be due to different mechanisms. Both *CHL1* and *CTF19* genes (red ellipses) have functions related to sister chromatid pairing during the S-phase. Thus, their aggravating interaction (denoted by a blue line) might be a result of their overlapping functions (left). However, the aggravating interactions of *CHL1* and *BUB3*, which is part of the spindle assembly checkpoint, is more likely the result of a different mechanistic reason (denoted by a directed red arrow; right), where the lack of a gene (i.e. *chl1Δ*) induces abnormal chromosome segregation, that requires the activation of the spindle assembly checkpoint including *BUB3*. (B) Yeast cells exposed to benomyl (denoted by a green diamond) show the same sensitivity to *BUB3* perturbation as the *chl1Δ* strain, suggesting that *chl1Δ* background causes a stress similar to exposure to benomyl.

microtubule depolymerizing agents (e.g. benomyl). In turn, the deletion strain of *bub3Δ* shows growth retardation under benomyl. Thus, we interpret the aggravating interaction between *CHL1* and *BUB3* as resulting from unidirectional compensation, where *CHL1* is the upstream gene and *BUB3* is the downstream gene (Fig. 6). Indeed, this interpretation is conceivable, as *Chl1* is involved in sister chromatid pairing during the S phase, and *Bub3* is part of the spindle assembly checkpoint, in charge of delaying anaphase in cases of abnormal spindle assembly.

When elaborating this reasoning we have to be careful not to confuse unidirectional compensation with *dosage effect*: if a gene phenocopies a stimulus, we might expect to see that its deletion amplifies the effect of this stimulus, showing higher sensitivity to its application (loosely stated, higher dosage of the stimulus). In such cases, we might mistakenly implicate an upstream gene to be downstream to another gene that also phenocopies the same stimulus. However, in such situations we will, by definition, identify bidirectional interactions where one gene is both upstream and downstream to another gene. Thus, we can detect these situations, and distinguish them from a proper unidirectional compensations.²

The reasoning we outline here (and apply below) detects, up to usual concerns about experimental or statistical noise, asymmetries of aggravating interactions with respect to phenotypes of external stimuli. This is a well-defined and clear criterion. A more ambitious step is to deduce from this asymmetry directionality in the underlying biological mechanisms. In our example of *CHL1* and *BUB3*, we have strong intuitions about the causal direction (as sister chromatid pairing precedes spindle assembly). In other cases, the underlying causality is much murkier. Moreover, we can imagine external perturbations that will lead to opposite asymmetry. For example, if a certain drug targets in a specific manner the spindle assembly checkpoint, we would detect asymmetric behavior of *CHL1* and *BUB3* to it, but in the opposite direction. This thought exercise implies that we need to be careful about deducing

²We estimate that up to five percent of unidirectional interactions are actually caused by dosage effect but were not identified as such since not all the genes were tested in all the screens (data not shown).

directionality in the underlying biology. However, we believe it is reasonable to assume that in most cases external perturbations are ones that causes cellular imbalances or stress conditions rather than disable mechanisms that cope with such situations.

3.2 Application to genetic interaction maps in *S.cerevisiae*

To systematically detect unidirectional compensation, we collected data from genetic screens that measured growth of yeast deletion strains under various external conditions and insults compared to YPD conditions (Bennett *et al.*, 2001; Dudley *et al.*, 2005; Giaever *et al.*, 2002; Hillenmeyer *et al.*, 2008; Parsons *et al.*, 2004, 2006). We considered deletion strains from both homozygote diploid and haploid deletions. We converted all measurements into a binary score, by defining genes with growth defects as those that passed the threshold defined by the authors of each study (for a detailed description of how we handled each dataset see Appendix B in the Supplementary website).

This process resulted in listing for each external stimulus the repertoire of deletion strains that display a growth defect in its presence. In a similar manner, each gene deletion defines a list of genes that are sensitive to its deletion, i.e. display aggravating interactions with it (using the same threshold, -2.5 , as Collins *et al.*, 2007a; Schuldiner *et al.*, 2005). We then define a unidirectional compensation between genes X and Y (associated with external perturbation P) if (i) there exists an aggravating interaction between X and Y ; (ii) the perturbation of Y leads to sensitivity to the external perturbation P ; (iii) X has aggravating interactions with a significant number of genes whose perturbations cause sensitivity to the perturbation P (using hyper-geometric test with FDR of 0.1); and (iv) at least one of the conditions 2 or 3 do not hold on the opposite direction (when switching the roles of X and Y).³

We applied this procedure to the CB and ESP genetic interaction maps and found 348 gene deletions that are phenocopied by at least one external stimulus. These stimuli include a wide range of external perturbations that match the nature of the specific data set analyzed. For example, many external stimuli corresponding to gene deletions in the CB map include agents causing DNA damage and microtubule depolymerization, while the stimuli related to the ESP map mostly include agents causing protein synthesis and glycosylation inhibition (see Supplementary website). To our surprise, more than one-third of the aggravating genetic interactions (CB: 4659/11539; ESP: 1036/2718) could be explained by unidirectional compensation.

4 ELUCIDATING THE FUNCTION OF CELLULAR PATHWAYS

We next asked whether unidirectional compensation can also be assigned within the modular hierarchy in terms of upstream and downstream modules. Toward this end, we incorporated these unidirectional interactions into our hierarchical organization of interacting modules. We annotated an aggravating edge between two modules as caused by unidirectional compensation if the majority

³To measure the statistical significance of the interactions we found, we created a random permutation of the names of the genes in the genetic interaction screen, and repeated the procedure described above. In 10 repeats, no significant overlaps between genes and external stimuli were found, thus no unidirectional interactions were identified.

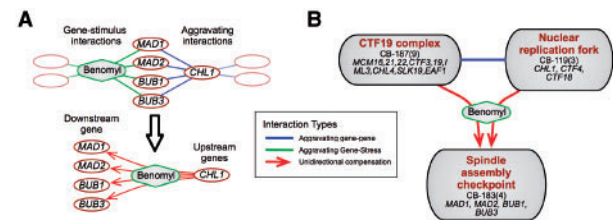
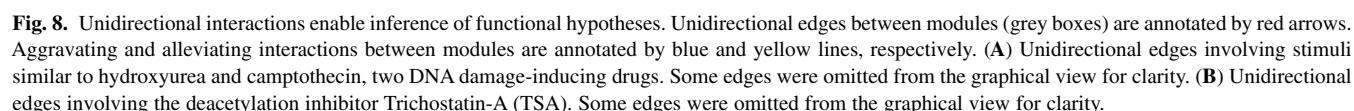


Fig. 7. Inter-module unidirectional interactions. **(A)** Systematic identification of unidirectional interactions: a systematic search discovers cases of statistically significant overlap between patterns of gene sensitivities under specific external stimuli (green lines) and the aggravating partners of specific genes (blue lines). We annotate these aggravating interactions as unidirectional, and denote them by red arrows directed from the upstream gene (whose deletion causes the cell perturbation) to the downstream genes (which deal with the particular cell perturbation). **(B)** All inter-module aggravating edges were scanned and searched for potential unidirectional edges. If the majority of the interactions involved in an inter-module aggravating edge are marked as consistent unidirectional interactions (corresponding to the same external stimulus and in the same direction), this edge was annotated as a unidirectional edge with respect to the specific external stimulus (green diamond).

of interactions between these modules are unidirectional and share the same context (i.e. have the same directionality and are related to the same external stimulus; Fig. 7A; Supplementary website). By requiring consistent unidirectional interactions between modules, this incorporation also removes potential errors in the annotation of unidirectional interactions (Supplementary website). We find that this designation elucidates the cellular role of modules and their interactions. Coming back to our previous example, we find that perturbations of modules CB-119 and CB-187 lead to stress conditions similar to those caused by microtubule de-polymerizing agent benomyl (Fig. 7B). Our analysis identified module CB-183 as downstream to benomyl-like stress caused by mutations of genes in CB-119 and CB-187. Indeed, the protein products of the genes in CB-119 and CB-187 are components of the machinery responsible for the correct distribution of chromosomes during cell division (Hanna *et al.*, 2001; Measday *et al.*, 2002). By de-polymerizing microtubules that create the spindle fibres, benomyl attacks a crucial component of this process. Finally, the genes in module CB-183 participate in the spindle assembly checkpoint that delays the onset of anaphase in cells with defects in mitotic spindle assembly (Nasmyth, 2005). This example demonstrates the power of our approach in automatically providing biological insights into the function of the genes in various modules.

The concise representation of the observed genetic interactions as edges within and between modules, in combination with the specific interpretation of many aggravating edges as caused by unidirectional compensations, pinpoints novel functions of modules that are not readily apparent from clustering of genetic interactions alone. The results of our automatic search provide an elaborate network of such inter- and intra-module edges, thus, we constructed a web-tool providing a user-friendly interface to browse our results in an effective manner (Supplementary website).

For example, examining unidirectional edges related to DNA damage agents, such as hydroxyurea and camptothecin, we find multiple upstream and downstream modules (Fig. 8A). A notable downstream module (CB-137) comprises three sub-modules; of



Another example regards the unidirectional edges related to TSA, a histone deacetylation inhibitor that affects class I and II histone deacetylases (Furumai *et al.*, 2001; Fig. 8B). We find two modules whose perturbation is phenocopied by TSA: Set3 complex (CB-82) and Thp1–Sac3 complex (CB-92). Set3 complex is a histone deacetylation complex, and thus it is plausible that TSA phenocopies its perturbation. However, the relation of the Thp1–Sac3 complex, comprising mRNA export factors associated with the nuclear pore, to deacetylation is less obvious. Clues to this puzzle can be found when examining the downstream modules with respect to this external stimulus. Most of these downstream modules are related to chromosome segregation (CB-121 and CB-183) and the Swr1 complex (CB-218), a chromatin modifier with genome integrity phenotype (van Attikum *et al.*, 2007). This suggests that TSA damages chromosome integrity, and that perturbations of Thp1–Sac3 complex and Set3 complex lead to similar damage. Indeed, previous studies showed that Thp1–Sac3 complex has a role in transcription elongation, and that its perturbation affects genome stability (González-Aguilera *et al.*, 2008). Previous works suggested

Our empirical results on two very different genetic interaction maps show that this representation captures much of the patterns of interactions in the data. Although our representation captures many interactions, it does not include all the interactions. Some of the missed interactions may be false positives, and thus at this front our analysis would serve to purge such data from the genetic interaction maps. There are, however, various reasons for missing

true interactions. For example, some interactions are excluded since we restrict the module size to at least two genes, so that noisy measurements for a specific deletion will not dominate the results. This implies that our procedure may miss a consistent set of interactions between a single gene and a module. Also, the constraint of a strict hierarchy may lead to situations where a gene with multiple functions has to choose which module to belong to and thus to miss some of its interactions (Pu *et al.*, 2008). A natural extension of our method, which can partially resolve this issue, is to allow an extended hierarchy, where a module can be the child of more than one parent. As demonstrated by the success of GO ontology in capturing functional annotations (Ashburner *et al.*, 2000), such hierarchical graphs are natural in the context of functional gene organization.

Striving for mechanisms: one goal of the analysis of genetic interaction maps is to decipher the causal explanation underlying the observed interactions. Automating this aspect of the analysis provides a significant advance toward interpretation of genetic interaction maps. Earlier studies mostly focused on interpretations that involve complexes and pathways (alleviating interactions among members of the complex/pathway, and a similar spectrum of interactions with other genes) and redundant functions of such complexes/pathways (parallel pathways may have aggravating interactions between genes involved in these pathways). Although other explanations were acknowledged (Boone *et al.*, 2007; Pan *et al.*, 2006) and implicitly used in interpreting the results, these were not reflected in automated analyses. Here, we introduce a novel automated analysis to systematically detect unidirectional interactions where a downstream gene buffers or compensates for the effect of the perturbation of an upstream gene.

Using our automated analysis, we find that a large portion of the observed aggravating genetic interactions (at least a third) can be attributed to such unidirectional interactions. This finding partially accounts for the large number of aggravating interactions between genes of distantly related functions. Moreover, the analysis annotates interactions by the type of damage caused by the perturbation of the upstream genes, providing informative clues for interpreting the results. Finally, we combine this analysis with the modular hierarchy representation to understand the relations between modules. When looking at the types of external stimuli phenocopied by gene deletions in our analysis, we find that many of them can cause major stress conditions in the cell such as DNA damage (e.g. by UV, hydroxyurea, camptothecin and MMS) and translation inhibition (e.g. cycloheximide and hygromycin B). In this case, we can interpret unidirectional compensations as connecting between a module whose perturbation causes stress and a module that has a part in relieving this stress. Indeed, many of the downstream modules associated with such stress conditions are known to be central players in the cellular response to various stress conditions, for example the DNA damage repair module (CB-137) and spindle assembly checkpoint (CB-183).

Global examination of the resulting network shows that many highly connected modules have a high percentage of their aggravating partners related through unidirectional edges related with major stress conditions (Fig. 9). Moreover, highly connected modules tend to be either upstream (i.e. their removal causes stress conditions) or downstream (i.e. stress relieving), but not both (Supplementary website). These observations suggest that

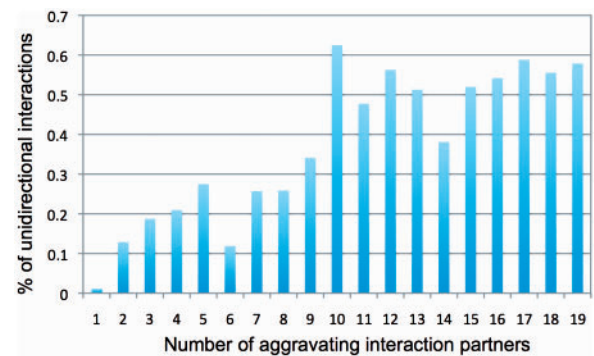


Fig. 9. Many hubs of genetic interactions are related to unidirectional compensation. A histogram of the fraction of unidirectional edges (y-axis) for modules with different degree of aggravating edges (x-axis). Each bar shows the portion of unidirectional edges out of all edges that are connected to modules with this degree.

unidirectional compensation plays a pivotal role in forming interaction hubs in genetic interaction maps. Furthermore, they suggest that responses of cellular integrity mechanisms to genetic perturbations are a major factor in shaping genetic interaction maps.

Toward organizational principles of genetic interaction maps: the methodology we present here puts forward two major contributions toward understanding the organization of genetic interaction maps. First, the hierarchy of modules is automatically built independent of additional data sources, allowing its application to various existing genetic interaction maps and also to less studied organisms. Moreover, the creation of a visual platform to study these results should boost the usability of these datasets, many of which are currently only used to find single interactions between genes of interest. Second, we elucidate some of the mechanisms underlying the interactions between modules. By integrating an additional data source we enabled the distinction between uni- and bi-directional aggravating interactions, and provided more functionally coherent interpretations to the genetic interaction maps. Our results demonstrate that searching for a causal explanation for the genetic interactions highlights specific insights into the cellular roles of genes and pathways as well as elucidates global features of the genetic interaction map. With the increasing availability of genetic interaction maps in yeast and as they become available for a large number of organisms, many of them with sparser annotation (Butland *et al.*, 2008; Byrne *et al.*, 2007; Roguev *et al.*, 2008), we believe that these methods can be generalized and will prove valuable in the automated highlighting of both the functional structure of the network as well as specific biological phenomena. This should allow us to make the first steps necessary to turn high-throughput maps into a true understanding of cellular complexity by interpreting how such maps relate to the underlying landscape of interacting cellular pathways.

ACKNOWLEDGEMENTS

We thank N. Barkai, S. Gasser, Z. Itzhaki, T. Kaplan, P.D. Kaufman, O.J. Rando, A. Regev, M. Yassour, E. Yeger-Lotem, I. Wapinski, and J.S. Weissman for discussions and useful comments on the article.

We also thank S. Collins and N. Krogan for making data available prior to publication.

Funding: Eshkol fellowship from the Israeli Ministry of Science (to A.J.); Rudin Foundation (to R.R.); Human Frontiers Science Program Career Development Award (to M.S.); European Union grant 3D-Repertoire, contract number LSHG-CT-2005-512028 (to H.M.); National Institutes of Health grant 1R01CA119176-01 (to N.F.).

Conflict of Interest: none declared.

REFERENCES

- Ashburner,M. *et al.* (2000) Gene ontology: tool for the unification of biology. The Gene Ontology Consortium. *Nat. Gen.*, **25**, 25–29.
- Bandyopadhyay,S. *et al.* (2008) Functional maps of protein complexes from quantitative genetic interaction data. *PLoS Comput. Biol.*, **4**, e1000065.
- Bennett,C.B. *et al.* (2001) Genes required for ionizing radiation resistance in yeast. *Nat. Gen.*, **29**, 426–434.
- Beyer,A. *et al.* (2007) Integrating physical and genetic maps: from genomes to interaction networks. *Nat. Rev. Genet.*, **8**, 699–710.
- Boone,C. *et al.* (2007) Exploring genetic interactions and networks with yeast. *Nat. Rev. Genet.*, **8**, 437–449.
- Butland,G. *et al.* (2008) eSGA: *E. coli* synthetic genetic array analysis. *Nat. Methods.*, **5**, 789–795.
- Byrne,A.B. *et al.* (2007) A global analysis of genetic interactions in *Caenorhabditis elegans*. *J. Biol.*, **6**, 8.
- Collins,S. *et al.* (2007a) Functional dissection of protein complexes involved in yeast chromosome biology using a genetic interaction map. *Nature*, **446**, 806–810.
- Collins,S. *et al.* (2007b) Toward a comprehensive atlas of the physical interactome of *Saccharomyces cerevisiae*. *Mol. Cell Proteomics*, **6**, 439–450.
- Cover,T. and Thomas,J. (2001) *Elements of Information Theory*. City College of New York, John Wiley, New York.
- Dudley,A. *et al.* (2005) A global view of pleiotropy and phenotypically derived gene function in yeast. *Mol. Syst. Biol.*, **1**, 2005.0001.
- Eisen,M. *et al.* (1998) Cluster analysis and display of genome-wide expression patterns. *Proc. Natl Acad. Sci.*, **95**, 14863–14868.
- Fiedler,D. *et al.* (2009) Functional organization of the *S. cerevisiae* phosphorylation network. *Cell*, **136**, 952–963.
- Furumai,R. *et al.* (2001) Potent histone deacetylase inhibitors built from trichostatin A and cyclic tetrapeptide antibiotics including trapoxin. *Proc. Natl Acad. Sci. USA.*, **98**, 87–92.
- Giaever,G. *et al.* (2002) Functional profiling of the *Saccharomyces cerevisiae* genome. *Nature*, **418**, 387–391.
- Glover,F. *et al.* (1993) A user's guide to TABU search. *Ann. Oper. Res.*, **41**, 1–28.
- González-Aguilera,C. *et al.* (2008) The THP1-SAC3-SUS1-CDC31 complex works in transcription elongation-mRNA export preventing RNA-mediated genome instability. *Mol. Biol. Cell.*, **19**, 4310–4318.
- Hanna,J. *et al.* (2001) *Saccharomyces cerevisiae* CTF18 and CTF4 are required for sister chromatid cohesion. *Mol. Cell Biol.*, **21**, 3144–3158.
- Helenius,A. and Aebi,M. (2004) Roles of N-linked glycans in the endoplasmic reticulum. *Annu. Rev. Biochem.*, **73**, 1019–1049.
- Hillenmeyer,M. *et al.* (2008) The chemical genomic portrait of yeast: uncovering a phenotype for all genes. *Science*, **320**, 362–365.
- Kelley,R. and Ideker,T. (2005) Systematic interpretations of genetic interactions using protein networks. *Nat. Biotech.*, **23**, 561–566.
- Kim,T. and Buratowski,S. (2009) Dimethylation of H3K4 by Set1 recruits the Set3 histone deacetylase complex to 5' transcribed regions. *Cell*, **137**, 259–272.
- Makhnevych,T. *et al.* (2009) Global map of SUMO function revealed by protein-protein interaction and genetic networks. *Mol. Cell*, **33**, 124–135.
- Masumoto,H. *et al.* (2005) A role for cell-cycle-regulated histone H3 lysine 56 acetylation in the DNA damage response. *Nature*, **436**, 294–298.
- Meadsday,V. *et al.* (2002) Ctf3p, the Mis6 budding yeast homolog, interacts with Mcm22p and Mm16p at the yeast outer kinetochore. *Genes Dev.*, **16**, 101–113.
- Nasmyth,K. (2005) How do so few control so many? *Cell*, **120**, 739–746.
- Pan,X. *et al.* (2006) A DNA integrity network in the yeast *Saccharomyces cerevisiae*. *Cell*, **124**, 1069–1081.
- Parsons,A. *et al.* (2004) Integration of chemical-genetic and genetic interaction data links bioactive compounds to cellular target pathways. *Nat. Biotechnol.*, **22**, 62–69.
- Parsons,A. *et al.* (2006) Exploring the mode-of-action of bioactive compounds by chemical-genetic profiling in yeast. *Cell*, **126**, 611–625.
- Pu,S. *et al.* (2008) Local coherence in genetic interaction patterns reveals prevalent functional versatility. *Bioinformatics*, **24**, 2376–2383.
- Rissanen,J. (1983) A universal prior for integers and estimation by minimum description length. *Ann. Stat.*, **11**, 416–431.
- Rogues,A. *et al.* (2008) Conservation and rewiring of functional modules revealed by an epistasis map in fission yeast. *Science*, **332**, 405–410.
- Schuldiner,M. *et al.* (2005) Exploration of the function and organization of the yeast early secretory pathway through an epistatic miniarray profile. *Cell*, **123**, 507–519.
- Segrè,D. *et al.* (2005) Modular epistasis in yeast metabolism. *Nat. Genet.*, **37**, 77–83.
- Suka,N. *et al.* (2001) Highly specific antibodies determine histone acetylation site usage in yeast heterochromatin and euchromatin. *Mol. Cell.*, **8**, 473–479.
- Tong,A. *et al.* (2001) Systematic genetic analysis with ordered arrays of yeast deletion mutants. *Science*, **294**, 2364–2368.
- Ulitisky,I. *et al.* (2008) From E-MAPs to module maps: dissecting quantitative genetic interactions using physical interactions. *Mol. Syst. Biol.*, **4**, 209.
- van Attikum,H. *et al.* (2007) Distinct roles for SWR1 and INO80 chromatin remodeling complexes at chromosomal double-strand breaks. *EMBO J.*, **26**, 4113–4125.
- Wang,A. *et al.* (2002) Requirement of hos2 histone deacetylase for gene activity in yeast. *Science*, **298**, 1412–1414.
- Wilmes,G.M. *et al.* (2008) A genetic interaction map of RNA-processing factors reveals links between sem1/dss1-containing complexes and mRNA export and splicing. *Mol. Cell*, **32**, 735–746.